Journal of Geoscience and Environment Protection, 2022, 10, 45-64
https://www.scirp.org/journal/gep
ISSN Online: 2327-4344
ISSN Print: 2327-4336

Groundwater Geochemistry and Saltwater Intrusion in the Dakar Coastal Area, Senegal

Ousmane Coly Diouf[1*], Lutz Weihermüller[2], Mathias Diedhiou[1], Edgar Y. Terence Benam Beltoungou[1], Ndeye Maguette Dieng[1], Seynabou Cissé Faye[1], Harry Vereecken[2], Serigne Faye[1]

[1]Geology Department, Faculty of Sciences and Techniques, Cheikh Anta Diop University of Dakar, Dakar, Senegal
[2]Forschungszentrum Jülich GmbH, Agrosphere Institute IBG-3, Jülich, Germany
Email: *ousmanecoly.diouf@ucad.edu.sn, *o.diouf@fz-juelich.de

How to cite this paper: Diouf, O. C., Weihermüller, L., Diedhiou, M., Beltoungou, E. Y. T. B., Dieng, N. M., Faye, S. C., Vereecken, H., & Faye, S. (2022). Groundwater Geochemistry and Saltwater Intrusion in the Dakar Coastal Area, Senegal. *Journal of Geoscience and Environment Protection, 10,* 45-64.
https://doi.org/10.4236/gep.2022.1012004

Received: October 18, 2022
Accepted: December 5, 2022
Published: December 8, 2022

Abstract

Groundwater levels and water samples were collected from 20 drinking water pumping and piezometer wells in the urban area of Dakar coastal region in the year 2019. The pH-value, electrical conductivity, as well as calcium, magnesium, sodium, potassium, chloride, sulfate, bicarbonate, and nitrate concentrations were measured to assess the hydrochemical quality of the infra-basaltic aquifer in the area. The present work carried out a hydrochemical analysis to interpret the groundwater chemistry of the aquifer. The results of this chemical analysis indicate that $Na^+ > Mg^{2+} > Ca^{2+} > K^+$ was the most dominant cation sequence in the groundwater, while $Cl^- > HCO_3^- > SO_4^{2-} > NO_3^-$ was the most dominant one for anions. The chemical analysis of our samples showed, that the Cl-Ca-Mg facies was dominant in the aquifer, while Cl-Na-K and HCO_3-Na-K facies represent 20% and 10% of the groundwater sampled, respectively. A comparison of the measured groundwater quality in relation to WHO drinking water quality standards revealed that 80% of the water samples are suitable for drinking purposes. Ca enrichment, Simpson ratio, ratio of sodium chloride, and calculating Base Exchange (BEX) indices for the samples revealed that the groundwater is mainly affected by three factors: seawater intrusion due to aquifer overexploitation on one hand, and freshening processes and nitrate pollution, on the other, mainly caused by the groundwater flow from the unconfined aquifer.

Keywords

Coastal Groundwater, Major Ions, Hydrochemical Facies, Anthropogenic Activities, Nitrate Pollution

1. Introduction

Groundwater is a vital resource for drinking water, especially in most arid and semi-arid regions worldwide where surface water is poor in quality and often scarce (Eissa et al., 2018; Li & Qian, 2018). It is estimated that globally more than 1.5 billion people rely on groundwater for primary needs such as drinking and irrigation (Adimalla & Li, 2019). In semi-arid regions, intense urbanization led to high water demands and as a consequence, large extraction of groundwater is observed in these regions. On the other hand, water quality often dropped over the last years due to population and industrial growth and associated pollution of the aquifer systems (Rosegrant et al., 2009; Isa et al., 2012; Adimalla & Li, 2019). Especially, coastal groundwater systems are prone to quality changes induced by seawater intrusion caused by over-exploitation or rising sea-level (Roy & Bithin, 2018; Lal & Bithin, 2019), paleo salinity, and changes of climatic conditions leading to health risks for the populations in coastal zones (Faye et al., 2005; Werner et al., 2017; Kumari et al., 2018; Chidambaram et al., 2018; Balamurugan et al., 2020; Prakash et al., 2020). Over the past several decades, deterioration of coastal groundwater quality due to over-exploitation has been studied widely (e.g., Revelle, 1941; Narayana & Suresh, 1989; Ramesh et al., 1995; Pulido-Leboeuf, 2004; Walraevens & Van Camp, 2005; Bahir et al., 2018; Eissa et al., 2018) and geochemical indicator methods were applied to understand the dynamic behavior of coastal aquifer chemistry (Pascual & Custodio, 1990; Dixon & Chiswell, 1992; Appelo & Postma, 2005; De Montety et al., 2008; Fadili et al., 2015; Maman Hassan, 2022; Bauer et al., 2022; Daniele et al., 2022).

Dakar City, which is the major seat of governmental institutions in Senegal, is the biggest urban agglomeration in Senegal and a major financial, commercial, manufacturing, and transport hub. The population of Dakar is about 3 million (ANSD, 2020), whereby steady rural-urban migration causes problems typical of substropical and tropical megacities. Among others, these problems include sluggish infrastructural growth and poor sanitation drainage.

In the early 1920s, the water supply in Dakar city was drawn by a few groundwater extraction wells from the infrabasaltic aquifer at a rate of ~3000 $m^3 \cdot d^{-1}$ (OMS, 1972) but the demographic expansion has led to an increase in water demand. Since the 1970s, the water supply of Dakar from local aquifers was no longer sufficient, and therefore, it was necessary to explore other resources to satisfy the urban and peri-urban water needs. Despite the exploitation of the Pout, Sebikotane, and Paleocene limestone aquifers, the north coast and the Maastrichtian groundwater's but also the Senegal River connected via pipeline to the 250 km far away Lake of "Guiers" (Keur Momar Sarr 1 and 2) were used for drinking water supply. Nevertheless, the Dakar region still experiences problems of water supply for domestic and industrial needs.

Reacting on the increasing water demand, a medium-long term program has been initiated consisting of the construction of a new water purification plant in 2021 (Keur Momar Sarr 3, KMS3) and seawater desalination plants, which will be operational in 2025, to provide a sustainable solution to this drinking water supply problem in Dakar city. However, to reduce the water deficit in the short-term, a program was initiated in 2014 consisting of drilling new boreholes into the infrabasaltic aquifer. As a result, the pumping rates of this aquifer increased from 12,000 to 42,489 $m^3 \cdot d^{-1}$ between 2006 and 2019. This groundwater pumping rate, which were around 18,000 $m^3 \cdot d^{-1}$ between 1960 and 1987 and 17,000 $m^3 \cdot d^{-1}$ between 1989 and 1995, were reduced to 12,000 $m^3 \cdot d^{-1}$ since 2006 due to the saltwater intrusion from the northern and southwestern part of the aquifer, (GKW, 2009). On the other hand, previous studies from the infrabasaltic aquifer (OMS, 1972; Gaye, 1980; Tandia et al., 1998; Tandia, 2000; GKW, 2009) showed that a pumping rate of 18,000 $m^3 \cdot d^{-1}$ represents the equilibrium rate with groundwater recharge with a minimum loss of freshwater of 2000 $m^3 \cdot d^{-1}$ towards the Atlantic Ocean.

The aim of the present study is therefore to determine the impact of the increase in groundwater extraction from the beginning of the year 2015 on the piezometric and hydrochemistry behavior of the infrabasaltic aquifer of the Dakar region. Thereby, the results can guide the effective management of the groundwater resources of the Dakar city and to mitigate the water deterioration quality.

2. Materials and Methods

2.1. Study Area

The Dakar region extends over 550 km^2 between 16˚55' - 17˚30' west and 14˚55' - 14˚35' north (**Figure 1**). The region is characterized by a semi-arid climate with a rainy season between June and October. Climatic data collected from the Senegal National Civil Aviation and Meteorological Agency (ANACIM) shows, that annual rainfall varies strongly between the years being for example 161 mm in 2014 and 723 mm in 2009, while the long-term mean is 378 mm (1990-2019). Maximum air temperature is on average 28.4˚C (1990-2019) and occurs from May to June and October to November corresponding to the beginning and the end of the rainy season. Minimum air temperature is observed during the period from December to February (21.9˚C). Daily mean FAO-PM reference evapotranspiration estimated between 2000 and 2013 ranged between 2 and 4 $mm \cdot d^{-1}$ (Diouf et al., 2016).

Geologically, the Dakar region belongs to the Senegalese-Mauritanian basin, the largest coastal basin of northwest Africa (Castalain, 1965), which is covered by Quaternary sediments of sandy and sandy clay nature from alluvial and eolien deposits (Bellion, 1987).

The Dakar area has two aquifers systems (Martin, 1970), a semi-confined infrabasaltic aquifer in the western part and the unconfined Thiaroye aquifer in the eastern part (**Figure 2**). The infrabasaltic aquifer is composed of pure sand capped by volcanic lavas (Quaternary volcanism), while the unconfined Thiaroye aquifer varies from coarse to clayey sand. The thickness of the confined

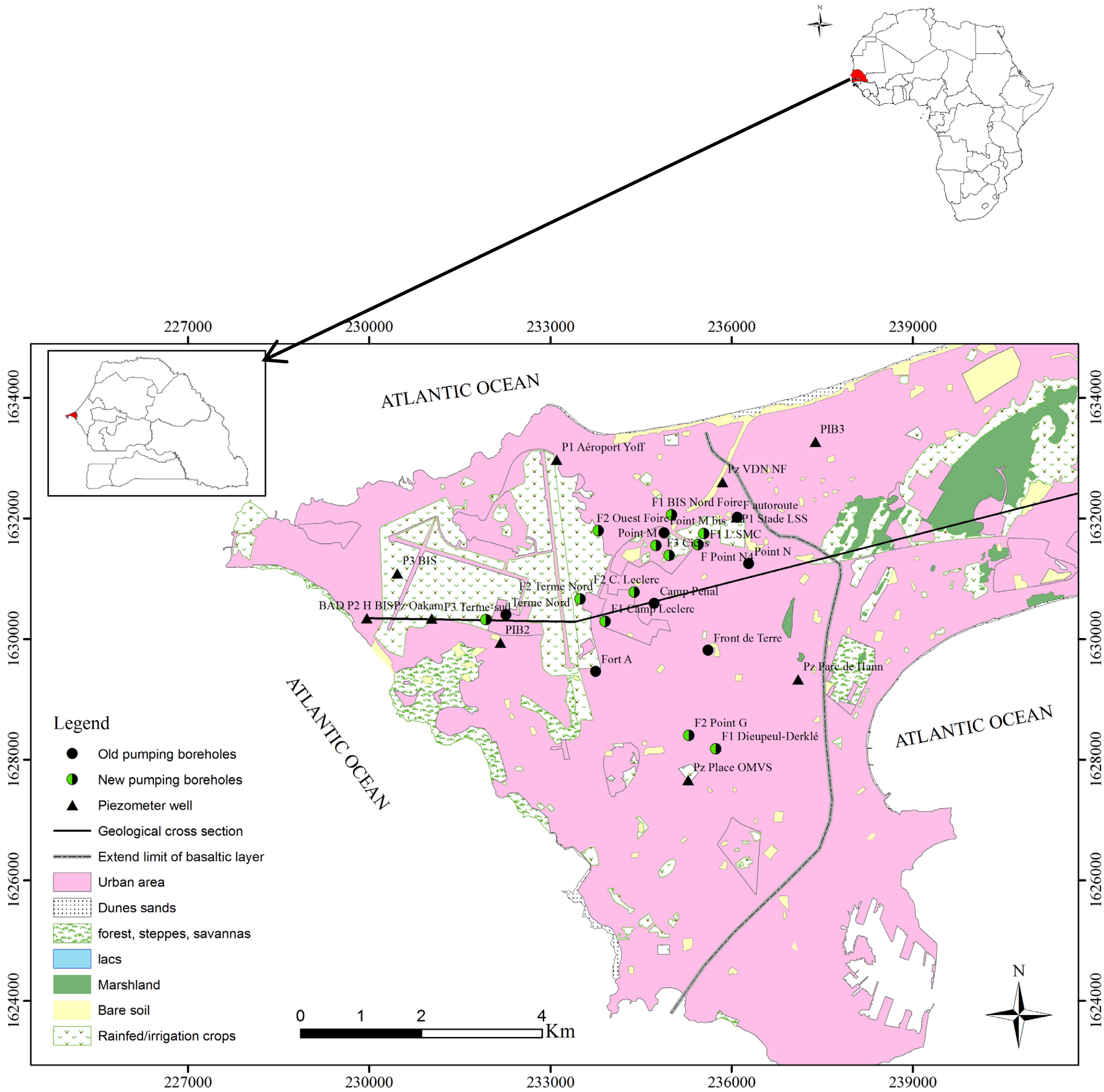

Figure 1. Land use, groundwater extraction and piezometer wells location in the study area of Dakar city.

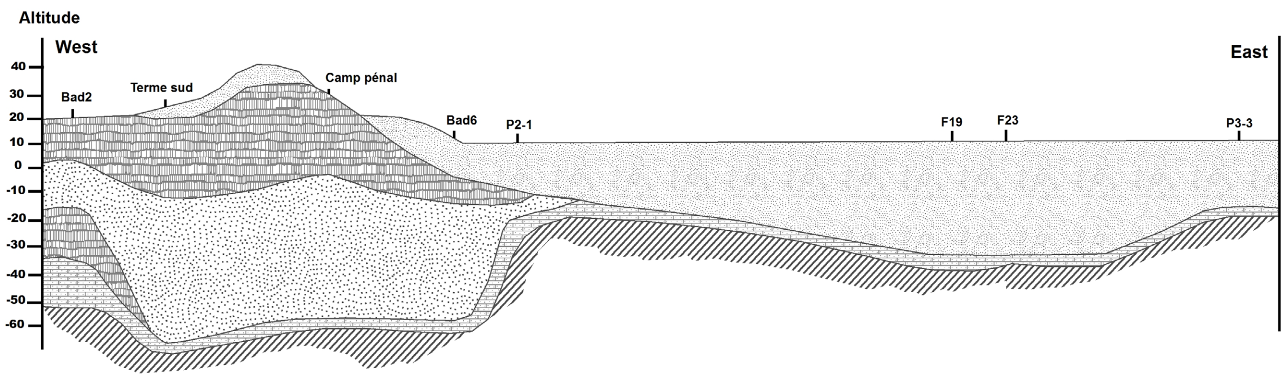

Figure 2. Hydrogeological section in the Dakar area (Chaoui, 1996).

aquifer varies from 50 to 80 meters from west to east. Previous studies using stable isotopes (Gaye, 1980) showed, that groundwater recharge by rainwater occurs mainly in the eastern parts between July to October. Some recharge could also occur through infiltration into the basaltic layer. Transmissivity values of the aquifer range from 9×10^{-3} to 10^{-2} $m^2 \cdot s^{-1}$ in the western part of the area (OMS, 1972).

2.2. Water Sampling, Field Data, and Laboratory Measurements

The groundwater sampling campaign was performed in June 2019 on a network of 20 groundwater extraction and piezometers wells (Figure 3) to determine the piezometric water levels and to sample the groundwater for the measurements of the physicochemical parameters. A GPS system was used to locate the exact coordinates of the sample location. Prior sampling of the groundwater at the piezometer wells pumping was carried out in order to obtain a representative sample. On the other hand, no extra pumping was performed at the groundwater extraction wells as they continuously pump water anyway. At each sampling point, two water samples were collected in polyethylene bottles and kept cool at 4˚C. Subsamples for cation analyzes were acidified to pH-values below 2 by adding HNO_3^- and the non-acidified samples were used for anion analyzes. All chemical analyses were performed at the chemistry laboratory of Geology Department of the Cheikh Anta Diop University of Dakar. Major ions were measured

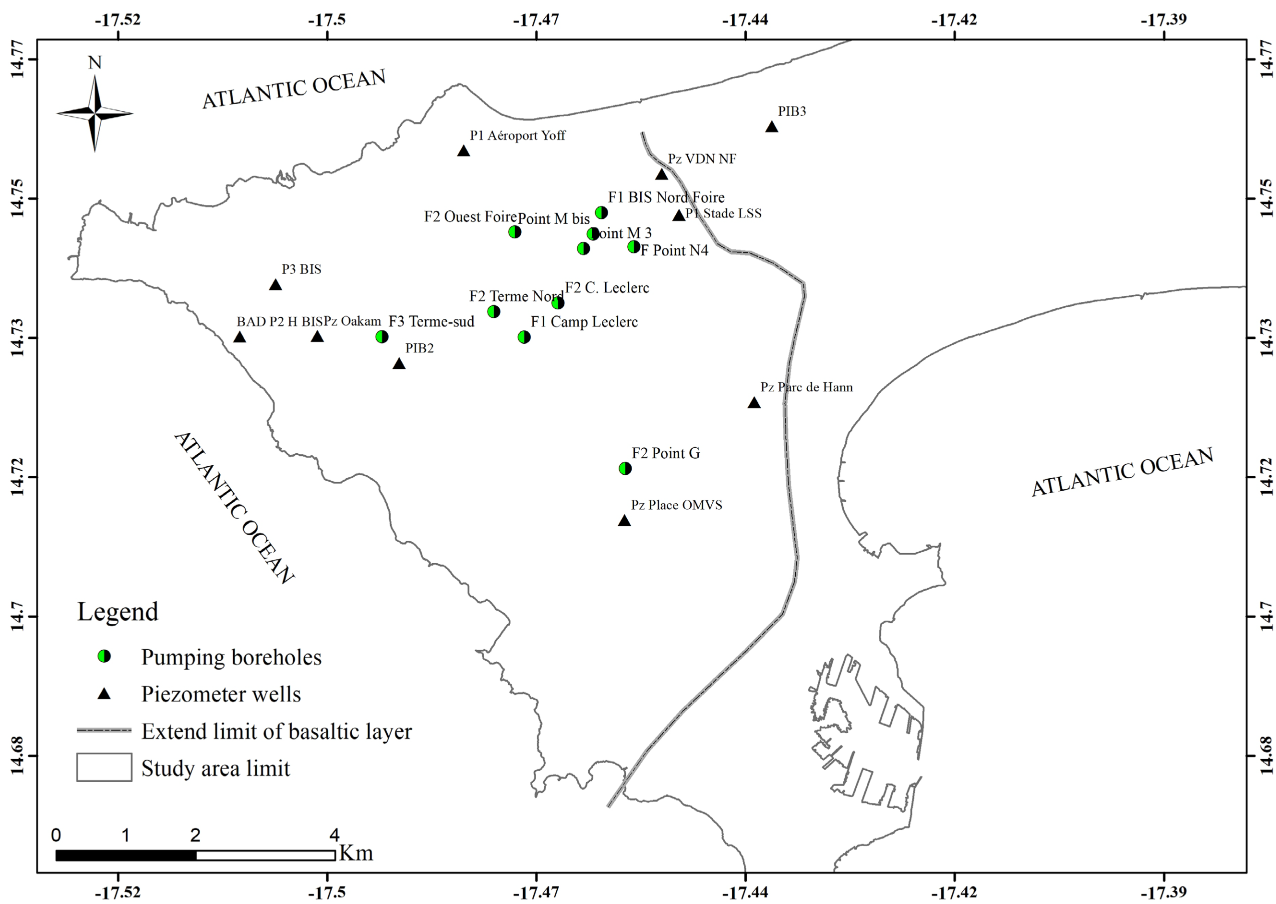

Figure 3. Location of the 20 sampling points in the study area.

by ion chromatography using a Dionex DX 120 (ThermoFischer Scientific). Physicochemical parameters such as pH-value, temperature, and electrical conductivity were determined *in situ* with a multi-parameter probe (WTC multi 3430 Set G). The depth of the groundwater table was measured using a light and sound piezometric probe (Type Delta-D 0100200S).

The piezometric maps of 1995 and 2009 were drawn using data collected from Chaoui (1996) and on the other hand from the PROGRESS database of the DGPRE (Water Resource Planning Department of Senegal).

In this study, the drinking water standards of World Health Organization (WHO, 2017) were used as the standard to determine the groundwater quality for drinking water purposes. On the other hand, total hardness, Ca enrichment, Simpson ratio, ratio of sodium chloride, and calculating Base Exchange Indices (BEX) were used as tools to evaluate potential saltwater intrusion (Klassen et al., 2014).

Total hardness (TH) was calculated from the values of the calcium and magnesium ion concentration in the groundwater samples according to Todd (1980).

$$\mathrm{TH} = 2.497 \times \mathrm{Ca}^{2+} + 4.115 \times \mathrm{Mg}^{2+}. \tag{1}$$

where Ca^{2+} and Mg^{2+} were expressed in mg·L^{-1}. TH values for water can be distinguished into four classes according to Sawyer & McCartly (1967). TH values less than 75 feature class I characterized by soft water, class II shows TH values between 75 and 150 and is characterized by moderately hard water, hard water have TH values between 150 and 300 (class III). Very hard water (class IV) exceeds TH values of 300.

The enrichment of Ca is expressed by Equation (2) according to Bear et al. (1999) and Moujabber et al. (2006) based on the ratio of Ca^{2+} and Mg^{2+}. High ratios of enrichment of Ca (>1) could be interpreted as saltwater intrusion as shown by Bear et al. (1999).

$$\text{Ca Enrichment} = (\mathrm{Ca}/\mathrm{Mg}). \tag{2}$$

whereby all ions are expressed in mg·L^{-1}.

The Simpson ratio (SR) provided by Equation (3) (Todd et al., 2005) is based on the Cl^{-}, HCO_3^{-}, and CO_3^{2-} concentrations expressed in mg·L^{-1}.

$$\text{Simpson Ratio} = \mathrm{Cl}^{-} \Big/ \left(\mathrm{HCO}_3^{-} + \mathrm{CO}_3^{2-}\right). \tag{3}$$

whereby the classification of groundwater according to the SR allows the definition of five classes (Todd et al., 2005): good quality (SR < 0.5), slightly contaminated (0.5 < SR < 1.3), moderately contaminated (1.3 < SR < 2.8), injuriously contaminated (2.8 < SR < 6.6), and highly contaminated (6.6 < SR < 15.5).

The ratio of sodium chloride (SCR) has often been used to identify the mechanism for acquiring salinity in semi-arid regions (Sami, 1992; Meybeck, 1987; Rogers, 1989).

$$\mathrm{SCR} = \mathrm{Na}^{+}/\mathrm{Cl}^{-} \tag{4}$$

whereby Na^{+} and Cl^{-} ion concentrations are in meq·L^{-1}.

Based on Bear et al. (1999), Marghade et al. (2012) proposed that saltwater intrusion show SCR less than 0.86, while SCRs larger 1 can be interpreted by anthropogenic sources of contamination. Between those two limits (0.86 and 1), the contamination process can be threshold by the mean value of 0.93. Therefore, if the values of SCR are less than 0.93, the contaminant source is likely related to saltwater intrusion and if the values exceed 0.93 it is likely caused by anthropogenic pollution.

The Base Exchange Indices (BEX) is calculated by Equation (5), whereby all ion concentrations are in meq·L^{-1}. According to Stuyfzand (2008) the BEX can be used to distinguish between salinization or freshening processes of an aquifer. Positive and negative values of BEX indicate respectively the freshening or the salinization process, and a value of zero indicates no base exchange.

$$\mathrm{BEX} = \mathrm{Na}^{+} + \mathrm{K}^{+} + \mathrm{Mg}^{2+} - 1.0716 \times \mathrm{Cl} \tag{5}$$

3. Results and Discussion

3.1. Impact of Pumping on the Groundwater Level

The piezometric maps of December 1995, June 2009, and December 2019 were used to describe the overall morphology of the groundwater and to characterize the groundwater flow directions. As can be seen from the equipotential lines, the overall morphology of the groundwater table has a depression formed by pumping at the main extraction points "Front de Terre" and "Camp Penal" close to the center of the study area. Hereby, the piezometric maps of December 1995 (**Figure 4(a)**) and June 2009 (**Figure 4(b)**), show in general the same pattern of the piezometric surface. In 1995, the groundwater pumping was 17.127 m^3·d^{-1} and the highest pumping rate were observed at "Point N", "Point M", "Terme Nord", "Fort A", "Front de Terre", and "Camp Penal" boreholes located in the central part of the aquifer. In 2009, the decrease of pumping from boreholes was up to 11.420 m^3·d^{-1}. Water level rising caused by this pumping decrease was much higher in "Front de Terre", "Camp Pénal", and "Fort A" boreholes, where the piezometric water level values are respectively −7, −4, and −3 m in 1995 and −4, −2, and −1 m in 2009. The groundwater flow is centripetal over the pumped boreholes zone, which makes it possible to highlight the influence of pumping on the piezometric water level. The piezometric map of December 2019 (**Figure 4(c)**) shows a different morphology compared to those observed in December 1995 and June 2009. In the Northern part of the study area the piezometric groundwater levels were lower than the sea water level. This piezometric depression is probably related to the increase of the pumping in this area, because in 2018 19 boreholes tapping the aquifer were functional extracting 34.890 m^3·d^{-1} of water. Among these 19 functional boreholes, 14 were located in the Northern part extracting 25.695 m^3·d^{-1} or ~74% of the total water. This piezometric depression is slightly oriented toward N-E. However, water levels rising occured in the piezometer PIB3 located in the north eastern part, where the aquifer is unconfined. This water level rising was likely caused by recharge coming from the

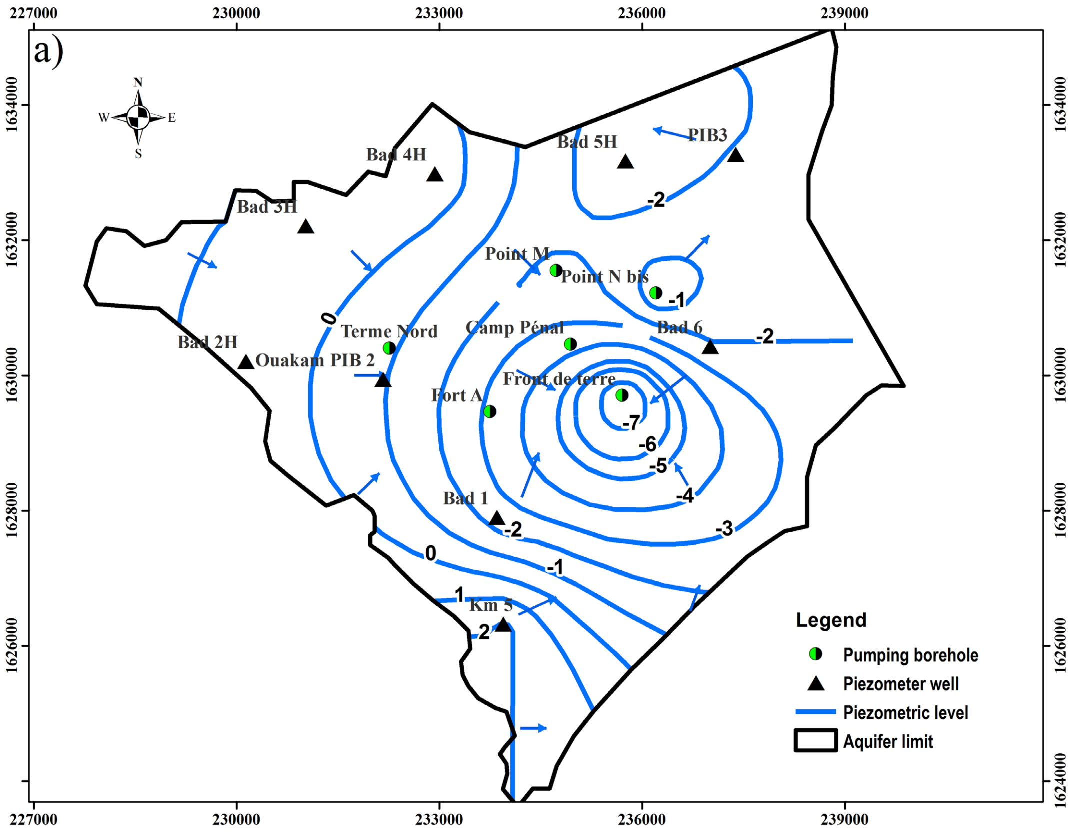

a)
Legend
Pumping borehole
Piezometer well
Piezometric level
Aquifer limit
Bad 5H
PIB3
Bad 4H
Bad 3H
Point M
Point N bis
Bad 2H
Terme Nord
Camp Pénal
Bad 6
Ouakam PIB 2
Front de terre
Fort A
Bad 1
Km 5

(a)

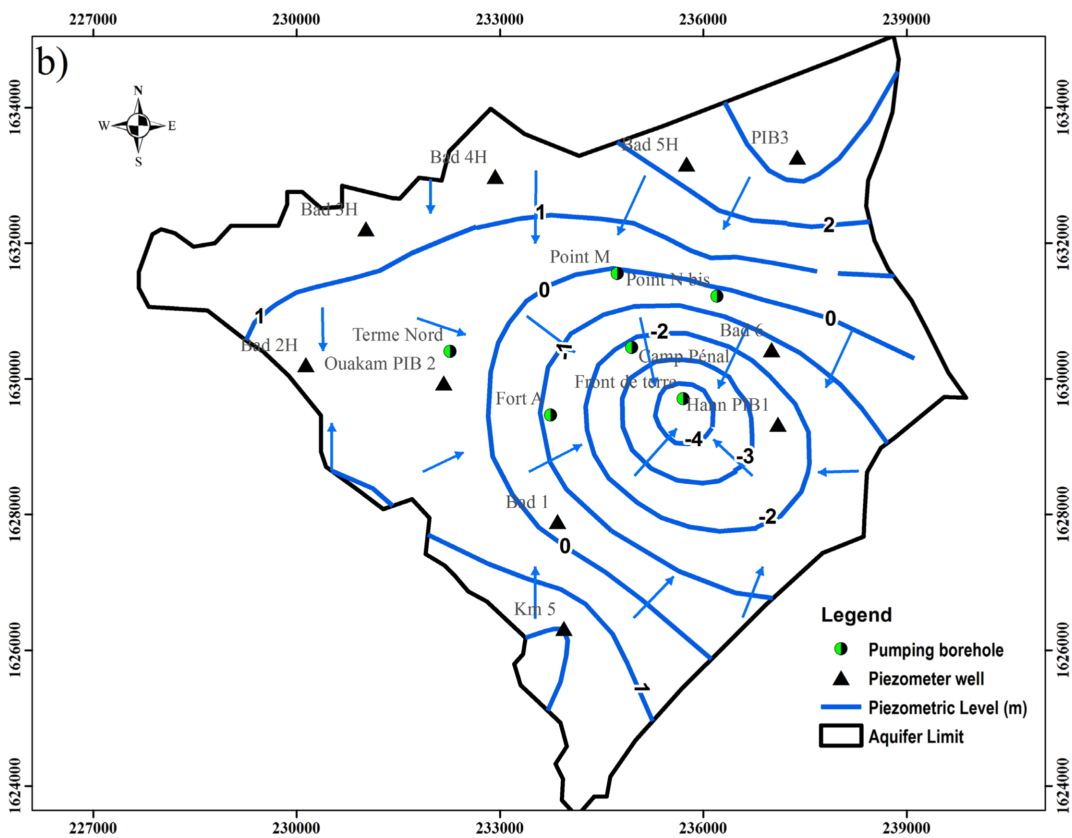

b)
Legend
Pumping borehole
Piezometer well
Piezometric Level (m)
Aquifer Limit
Bad 5H
PIB3
Bad 4H
Bad 3H
Point M
Point N bis
Bad 2H
Terme Nord
Ouakam PIB 2
Camp Pénal
Bad 6
Front de terre
Fort A
Hann PIB1
Bad 1
Km 5

(b)

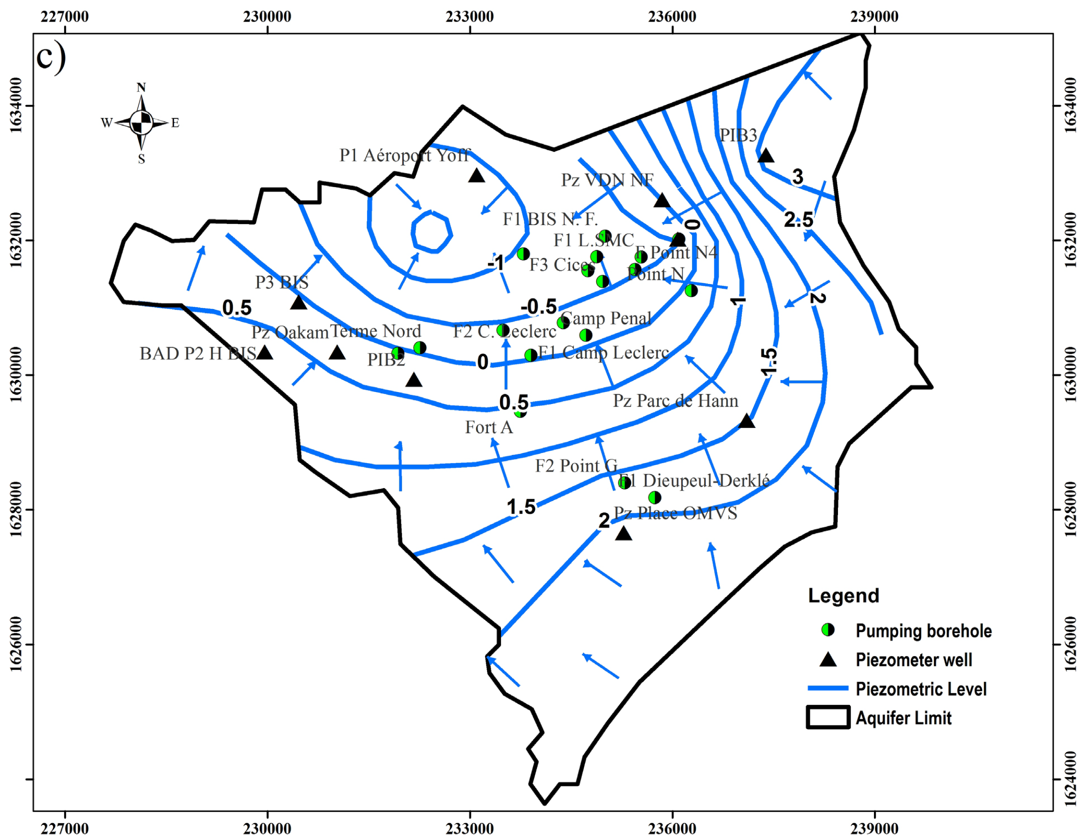

(c)

Figure 4. Groundwater level contours of the infrabasaltic aquifer (a) in December 1995; (b) in June 2009; and (c) in December 2019.

eastern part (groundwater flow from the Thiaroye unconfined sandy aquifer). Towards the south-east, water level rising was also observed, which can be explained by a decrease in pumping in this area and the direct infiltration of rainwater due to the low thickness or absence of the basaltic cover. In summary, the comparison of the piezometric maps of December 1995 and December 2019 showed that the piezometric depression located in the central part of the aquifer ("Front de Terre", "Camp Penal", and "Fort A" boreholes) in December 1995 has migrated towards the northern part in December 2019. This migration of the groundwater depression is accompanied by a slight water level rise in the south-eastern part of the study area.

3.2. Groundwater Chemistry

3.2.1. General Groundwater Characterization

The hydrogeochemical analysis of the groundwater samples showed, that several major ions play a significant role in the groundwater chemistry. The dominant ions found were Cl^-, Na^+, Mg^{2+}, and HCO_3^- and an overview of the chemical composition of the groundwater samples in the study area are summarized in Table 1.

In general, the dominant cations and anions in fresh groundwater are Ca^{2+}

Table 1. Summary statistics of the infrabasaltic groundwater quality parameters sampled in June 2019. Highlighted are those parameters exceeding the WHO standards in the mean values.

Variables	Unit	Mean	Median	Minimum	Maximum	WHO international standards (2017)
pH	-	7.24	7.18	6.51	7.87	6.5 - 8.5
Temperature	˚C	30.6	30.7	29.0	32.0	-
EC	($\mu S \cdot cm^{-1}$)	**3270.2**	792.5	365.0	37181.9	1000
TH	($mg \cdot L^{-1}$)	446.9	250.6	81.2	2700.2	100 - 500
HCO_3^-	($mg \cdot L^{-1}$)	**132.8**	116.0	18.0	348.0	10
Cl^-	($mg \cdot L^{-1}$)	**1096.4**	145.3	67.94	14574.0	200
SO_4^{2-}	($mg \cdot L^{-1}$)	55.2	16.0	6.0	232.0	250
NO_3^-	($mg \cdot L^{-1}$)	34.5	12.6	0.0	292.0	50
Na^+	($mg \cdot L^{-1}$)	**516.6**	72.5	23.0	8557.0	200
K^+	($mg \cdot L^{-1}$)	17.27	6.15	1.83	213.0	50
Ca^{2+}	($mg \cdot L^{-1}$)	79.1	45.3	17.6	410.8	75 - 200
Mg^{2+}	($mg \cdot L^{-1}$)	60.5	22.7	7.0	479.0	50 - 150

and HCO_3^- or SO_4^{2-}. However, in groundwater samples affected by seawater intrusion the order of magnitude of cations (Na^+, K^+, Ca^{2+}, Mg^{2+}) and anions (Cl^-, SO_4^{2-}, HCO_3^-) changes (Hoyle, 1990; Bouderbala, 2015). The sequence of major ion found in the groundwater sampled (expressed in $meq \cdot L^{-1}$) indicate a general order from $Na^+ > Mg^{2+} > Ca^{2+} > K^+$ for the cations and $Cl^- > HCO_3^- > SO_4^{2-} > NO_3^-$ for the anions. This sequence of cations and anions showed that the infrabasaltic groundwater is in general affected by saltwater intrusion. The concentration of each major ion was plotted into the Piper diagram (**Figure 5**) to identify the facies of groundwater in the study area. This diagram can be also used to determine the area affected by saltwater intrusion (Bouderbala, 2015). The diagram consists of three well-defined fields, two triangular fields (cation and anion) and an above central diamond-shaped field. The overall characteristics of water were inferred in this above central diamond-shaped field by projecting the position of plots in the triangular fields (Piper, 1944). The above central diamond-shaped field displays three groundwater facies such as Cl-Ca-Mg waters, Cl-Na-K waters, and HCO_3-Na-K waters. The most dominant water facies for our study area is the Cl-Ca-Mg water found in 14 boreholes (**Figure 5**). The position of Pz Parc Hann, P3 Bis, Pz VDN NF, P1 stade LSS, Pz Ouakam, and Pz place OMVS piezometer wells in the Piper diagram can be interpreted as affected by saltwater intrusion.

3.2.2. Drinking Water Quality

Depending on the specific standards of the water quality, its suitability for drinking purposes can be determined, whereby in this study the World Health Organization (WHO, 2017) drinking water standard were used to determine groundwater quality for drinking purposes (**Table 1**).

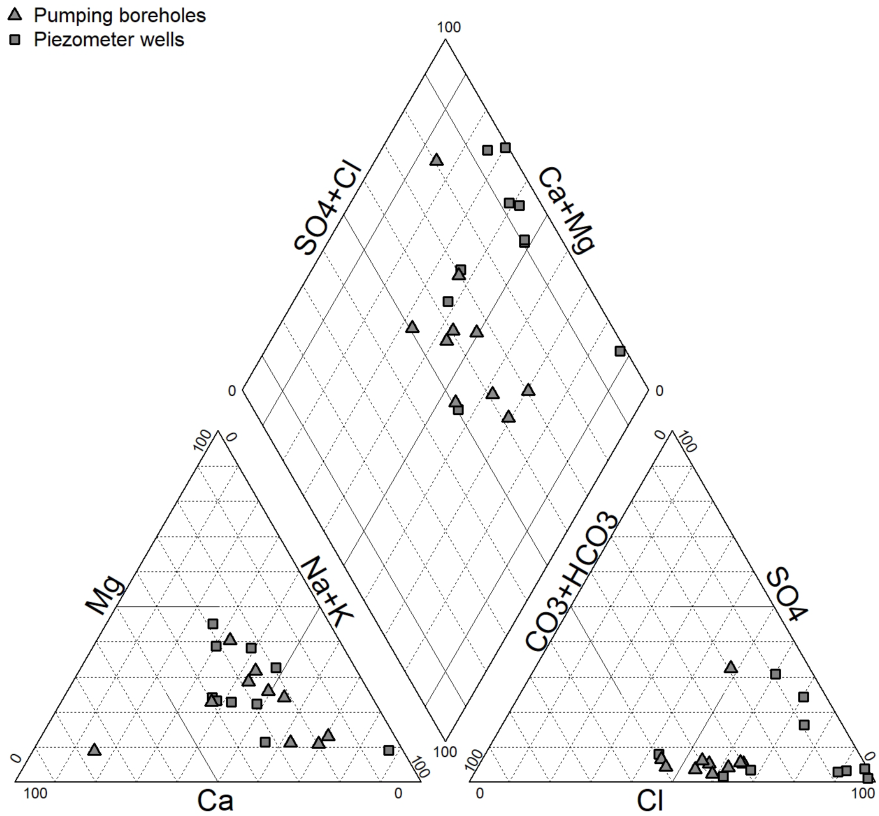

Figure 5. Piper diagram of the samples from the infrabasaltic aquifer.

In general, the pH-value is used to determine the acidity or alkalinity of the water. For drinking use, the pH-value must be between 6.5 and 8.5 (WHO, 2017). The pH-values of the infrabasaltic water samples varies between 6 and 8, thus showing that these waters, which are mostly alkaline, are in the range of drinking waters as recommended by WHO.

High EC contents in groundwater may cause gastrointestinal irritation in humans (Srinivas et al., 2013), and therefore, EC is also a critical measure for drinking water. The EC of the groundwater in the study area ranged between 365 and 37181 μS·cm^{-1} with a mean and median of 3270 and 793 μS·cm^{-1}, respectively, indicating that the groundwater samples exceed the WHO recommended limit of 1000 μS·cm^{-1} in the mean. Hereby, 35% of the water samples had EC values above the WHO threshold. Saxena et al. (2004) and Mondal et al. (2009) classified also water on the basis of EC into three categories: freshwater (<1500 μS·cm^{-1}), brackish water (1500 - 3000 μS·cm^{-1}), and saline water (>3000 μS·cm^{-1}). Based on this classification, 70% and 20% of the water samples fall within the fresh and brackish water classes, respectively. Only samples from piezometer "Parc Hann" and "Pz Quakam" (Cité Cheihk Amar) with extreme EC values of 37,182 and 11,590 μS·cm^{-1} are saline water.

Water total hardness (TH) is caused primarily by the presence of cations such as Ca^{2+} and Mg^{2+}. In the water samples analyzed, the TH varies between 81.2 to 2700 mg·L^{-1}, meaning that moderately hard, hard, and very hard waters were represented by 25%, 45%, and 30% of the groundwater samples.

The origin of nitrates in groundwater is mainly from anthropic activities such as agriculture and domestic wastewater and corresponding leaching from the soil surface (Kass et al., 2005; Schiavo et al., 2006). The nitrate contents in groundwater sampled in the area range from 0 to 292 mg·L^{-1}, whereby the WHO threshold for drinking water is set to 50 mg·L^{-1}. Out of the total 20 samples, two exceed the WHO threshold. Those piezometer wells where the nitrate content is extremely high with 292 and 124 mg·L^{-1} (P1 Stade LSS and PIB 3) were located in the eastern part of the study area and the reason for the high concentrations is probably the groundwater inflow from the unconfined Thiaroye aquifer. In the Thiaroye aquifer, measured nitrate concentrations rapidly increased over the last decades mainly caused by the expansion of unplanned urbanization and the infiltration of domestic wastewater into the groundwater due the poor sanitation system in the peri-urban areas. Nitrate values in Thiaroye aquifer varies between 5 to 34 mg·L^{-1} between 1966 and 1972 and presently reach an average of 400 to 450 mg·L^{-1} (Diédhiou et al., 2011; Diouf et al., 2012; Diaw et al., 2020; Pouye et al., 2022).

3.2.3. Saltwater Intrusion by Chemical Characterization and Indices

For the analysis of the saltwater intrusion, the enrichment of Ca, the SCR, the Simpson ratio, and the BEX were calculated and listed in **Table 2**.

Looking at the groundwater enrichment with Ca^{2+}, it was found, that 85.0% of the groundwater samples are affected by saltwater intrusion as the Ca^{2+} enrichment ratio exceeds 1, while the rest of the samples were affected by other processes reflected by ratios smaller 1. Those samples indicating other processes are taken from the piezometer wells Pz Parc Hann, P3 BIS, and Pz VDN NF.

The chloride and bicarbonate ratio values were used to calculate the Simpson ratio (SR) and showed that the infrabasaltic aquifer exhibits SR values ranging between 0.5 and extremely 66,419 with a median of 1.25 (**Table 2**). Based on this indice, the groundwater samples were classified into four classes (slightly to highly contaminated) with 60% exhibiting slightly sea water contaminated water (class II), followed by class V with highly contaminated state (20%) observed in Pz Parc Hann, P1 Stade LSS, Pz Place OMVS, Pz Oakam, and Pz VDN NF piezometer wells. Moderately and injuriously contaminated classes (class III and IV) are found respectively in PIB2, F2 Point G (10%), and PIB3 as well as in P3 BIS (10%).

The SCR can often been used to evaluate the degree of saltwater intrusion in groundwater (Sami, 1992; Meybeck, 1987; Rogers, 1989; Bear et al., 1999; Ben Moussa et al., 2011; Bouderbala, 2015; Putra et al., 2021). The dissolution of halite in water releases equal concentration of Na^{+} and Cl^{-} into the solution, but the analytical results presented in **Table 2** deviates from the equilibrium caused by natural processes, which is probably due to impacts of anthropogenic activities or saltwater intrusion on the groundwater system. Based on the SCR about 70% of the groundwater samples have SCR values less than 0.93 showing

Table 2. Saltwater intrusion analysis for groundwater sampled boreholes (SWI = saltwater intusion; Anthrop = anthropogenic pollution).

Well name	Ca Enrichement	Remark	Simpson Ratio	Remark	Sodium Chloride Ratio	Remark	BEX	Remark	Overall Remark
Point M bis	3.000	SWI	0.854	Slightly	1.345	Anthrop	1.429	Freshening	More Freshening Process
Point M 3	2.100	SWI	1.272	Slightly	1.090	Anthrop	1.076	Freshening	More Freshening Process
BAD P2 H BIS	4.722	SWI	0.500	Slightly	1.305	Anthrop	3.035	Freshening	More Freshening Process
Pz Parc Hann	0.609	No SWI	41.879	Highly	0.905	SWI	−23.439	Salinization	More SWI Process
F1 BIS Nord Foire	3.857	SWI	0.877	Slightly	1.023	Anthrop	0.506	Freshening	More Freshening Process
PIB2	2.708	SWI	1.357	Moderately	0.535	SWI	−0.743	Salinization	More SWI Process
PIB3	2.157	SWI	4.580	Injuriously	0.803	SWI	0.669	Freshening	More SWI Process
P1 Stade LSS	2.551	SWI	7.222	Highly	1.150	Anthrop	2.829	Freshening	Not defined
P1Aéroport Yoff	2.750	SWI	0.978	Slightly	0.611	SWI	−0.193	Salinization	More SWI Process
Pz Place OMVS	1.055	SWI	9.543	Highly	0.123	SWI	−13.560	Salinization	More SWI Process
Pz Oakam	1.325	SWI	66.419	Highly	0.169	SWI	−79.199	Salinization	More SWI Process
P3 BIS	0.989	No SWI	3.769	Injuriously	0.537	SWI	−1.062	Salinization	More SWI Process
Pz VDN NF	0.976	No SWI	6.680	Highly	0.538	SWI	0.398	Freshening	Not defined
F2 Terme Nord	1.482	SWI	0.518	Slightly	1.060	Anthrop	1.143	Freshening	More Freshening Process
F2 Point G	14.145	SWI	1.431	Moderately	0.249	SWI	−2.392	Salinization	More SWI Process
F2 Ouest Foire	1.627	SWI	0.730	Slightly	0.894	SWI	1.317	Freshening	More Freshening Process
F6 C. Leclerc	1.098	SWI	0.544	Slightly	0.783	SWI	2.372	Freshening	More Freshening Process
F Point N4	1.293	SWI	0.795	Slightly	0.762	SWI	0.597	Freshening	More Freshening Process
F3 Terme-sud	1.561	SWI	1.044	Slightly	0.745	SWI	0.451	Freshening	More Freshening Process
F1 Camp Leclerc	2.908	SWI	1.218	Slightly	0.536	SWI	−0.038	Salinization	More SWI Process

contamination by saltwater intrusion (SWI), while the other 30% with SCR values higher than 0.93 are interpreted as being affected by anthropogenic processes.

Finally, the BEX values were also used to identify the salinization or freshening process in the groundwater system studied. Positive BEX values were found in 60% of the groundwater samples indicating a freshening process. On the other hand, the remaining 40% of the samples provide strong indication of seawater intrusion, as indicated by negative BEX values.

The salinization process were observed in piezometers wells Pz Parc Hann, PIB2, P1 Aéroport Yoff, Pz Place OMVS, Pz Oakam, and P3 BIS as well as pumping wells F2 Point G, and F1 Camp Leclerc.

3.2.4. Delineation of the Saltwater Intrusion Areas

In an overall assessment of the saltwater intrusion (SWI), the water samples were classified by combining all the calculated indices (Ca^{2+} enrichment, Simpson ratio, SCR, and BEX) in order to determine the processes affecting the groundwater. A comparison between the indices showed similarities and relationships between the indices. However, disagreement of the result compares to one method with another was observed in some wells as well. For example, all calculated indices showed SWI in Pz Parc Hann, P3 Bis, and Pz VDN NF except the Ca enrichment who indicated no SWI in these groundwater extraction wells. Therefore, the overall combined SWI assessment was obtained when at least three of the calculated four indices showed the same classification of freshening or SWI.

By applying this method, SWI was observed in 40% of the groundwater samples. The saltwater intrusion zone (**Figure 6**) was mainly located in the northeastern and the southeastern part of the study area. In the northeastern, saltwater intrusion can be related to the piezometric depression caused by the overpumping of the boreholes located in this area. The same observation was shown in the previous works of GKW (2009), who indicate that the northeastern and the southeastern part of the study area are more sensitive to saltwater intrusion. The saltwater intrusion zone located in the central-western part is surrounded by a freshening area probably related to an upconing phenomenon because the piezometer well BAD P2 H BIS tapping the upper part of the aquifer is characterized by a freshening process. The freshening process was the most dominant process observed in the central part of the aquifer, whereby in this area also indications of contamination from anthropogenic activity were found probably introduced by lateral groundwater flow from the eastern part.

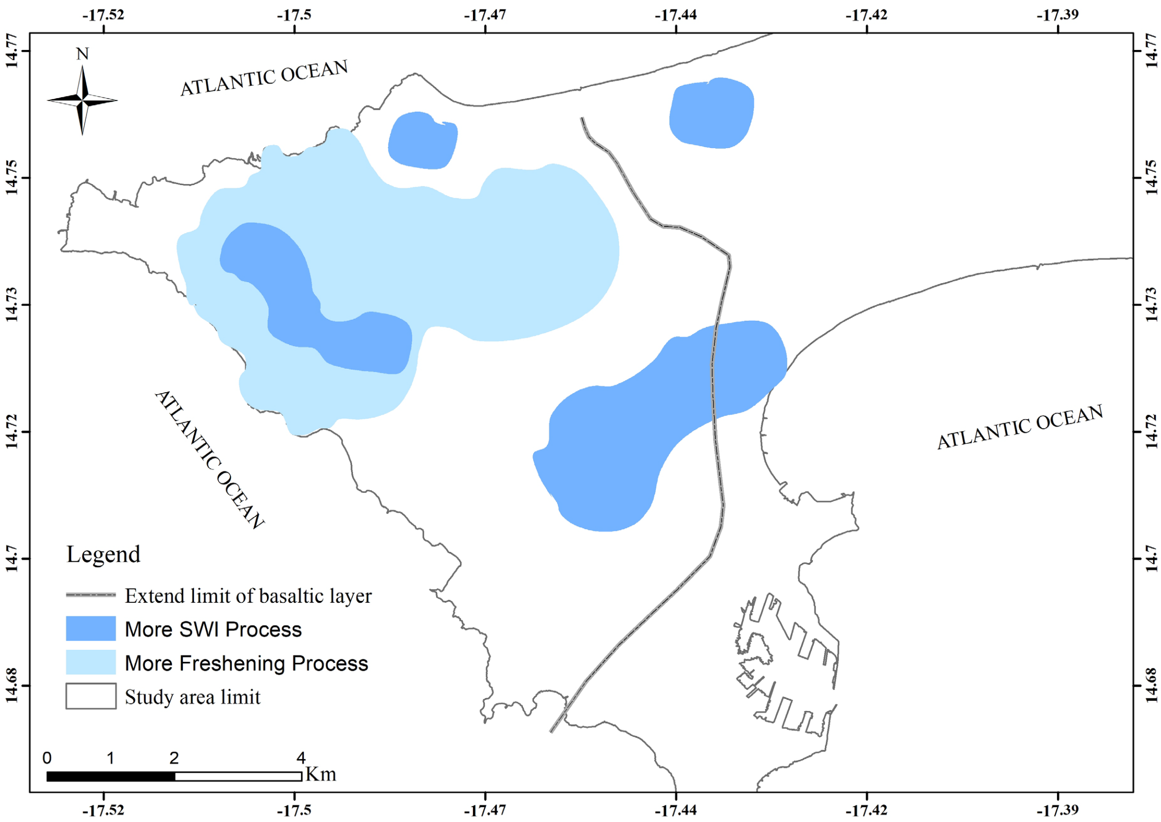

Figure 6. Saltwater intrusion zone map in the study area.

4. Conclusion

The area studied is underlain by a semi-confined aquifer composed of pure sand capped by volcanic lavas (quaternary volcanism), whereby overexploitation in the past years might have caused saltwater intrusion into the aquifer. The results of this study showed, that 80% of the groundwater samples are suitable for drinking and domestic use based on the World Health Organization drinking water thresholds. The Piper diagram showed the occurrence of several groundwater facies such as Cl-Ca-Mg, Cl-Na-K, and HCO_3-Na-K waters. The analysis of the saltwater intrusion phenomenon using the Ca enrichment, the SCR, the Simpson ratio and the BEX showed a similar process in each groundwater well. Hereby, 50 % of the groundwater samples experienced a freshening process. On the other hand, several wells provide strong evidences of saltwater intrusion, whereby the mode of intrusion depends on the sampling location. In the central part of the area, the saltwater intrusion seems to be caused by an upconing process. However, the infrabasaltic aquifer is more vulnerable to saltwater intrusion from the coastline in the southeastern and northeastern part. Further groundwater isotope study needs to perform to analyze groundwater-seawater interaction. According to the overall assessment of the study area, groundwater pumping of the infrabasaltic aquifer has to be reduced for future planning and management of SWI in this coastal aquifer.

Acknowledgements

The authors express gratitude to the anonymous reviewers whose comments contributed to perfecting this manuscript.

Author Contributions

Conceptualization, O.C.D and L.W.; Methodology, O.C.D. and L.W.; Software, O.C.D. and N.M.D.; Validation, H.V. and S.F.; Formal analysis, O. C.D. and L.W; Investigation, L.W., M.D. and S.C.F. Visualization, S.F. and H.V.; supervision, L.W., H.V. and S.F.

Consent for Publication

All authors have read and agreed to the published version of the manuscript.

Conflicts of Interest

The authors declare no conflict of interest.

References

Adimalla, N., & Li, P. (2019). Occurrence, Health Risks, and Geochemical Mechanisms of Fluoride and Nitrate in Groundwater of the Rock-Dominant Semi-Arid Region, Telangana State, India. *Human and Ecological Risk Assessment, 25,* 81-103. https://doi.org/10.1080/10807039.2018.1480353

ANSD (2020). *Situation économique et sociale du Sénégal.* Edition 2017-2018 (411 p.). ANSD.

Appelo, C. A. J., & Postma, D. (2005). *Geochemistry, Groundwater and Pollution* (2nd ed., p. 649). CRC Press. https://doi.org/10.1201/9781439833544

Bahir, M., Salah, O., & Paula, M. C. (2018). Geochemical and Isotopic Approach to Decrypt the Groundwater Salinization Origin of Coastal Aquifers from Semi-Arid Areas (Essaouira Basin, Western Morocco). *Environmental Earth Sciences, 77,* Article No. 485. https://doi.org/10.1007/s12665-018-7663-4

Balamurugan, P., Kumar, P. S., Shankar, K., Nagavinothini, R., & Vijayasurya, K. (2020). Non-Carcinogenic Risk Assessment of Groundwater in Southern Part of Salem District in Tamil Nadu, India. *Journal of the Chilean Chemical Society, 65,* 4697-4707. https://doi.org/10.4067/S0717-97072020000104697

Bauer, J., Borsig, N., Pham, V. C., Hoan, T. V., Nguyen, H. T., & Norra, S. (2022). Geochemistry and Evolution of Groundwater Resources in the Context of Salinization and Freshening in the Southernmost Mekong Delta, Vietnam. *Journal of Hydrology: Regional Studies, 40,* Article ID: 101010. https://doi.org/10.1016/j.ejrh.2022.101010

Bear, J., Alexander H. D. C., Shaul S. et al. (1999). *Seawater Intrusion in Coastal Aquifers: Concepts, Methods and Practices*. Kluwer Academic.

Bellion, Y. J. C. (1987). *Historique géodynamique post-paléozoïque de l'Afrique de l'ouest d'après l'étude de quelques bassins sédimentaires (Sénégal, Taoudenni, Iullemmeden, Tchad).* Ph.D. Thesis, Université d'Avignon.

Ben Moussa, A., Zouari, K., & Marc, V. (2011). Hydrochemical and Isotope Evidence of Groundwater Salinization Processes on the Coastal Plain of Hammamet-Nabeul, North-Eastern Tunisia. *Physics and Chemistry of the Earth, Parts A/B/C, 36,* 167-178. https://doi.org/10.1016/j.pce.2010.03.039

Bouderbala, A., (2015). Groundwater Salinization in Semi-Arid Zones: An Example from Nador Plain (Tipaza, Algeria). *Environmental Earth Science, 73,* 5479-5496. https://doi.org/10.1007/s12665-014-3801-9

Castalain, J. (1965). Aperçu stratigraphique et micropaléontologique du bassin du Sénégal. Historique de la découverte paléontologique. In *Collection de micropaleontology* (pp. 357-365). Dakar et mémoire, BRGM.

Chaoui, S. (1996). *Hydrogéologie et hydrochimie de la presqu'île du Cap-Vert (nappe infrabasaltique et nappe de Thiaroye) Sénégal.* Office de la recherche Scientifique et Technique Outre-mer (ORSTOM).

Chidambaram, S., Sarathidasan, J., Srinivasamoorthy, K., Thivya, C., Thilagavathi, R., Prasanna, M. V., Singaraja, C., & Nepolian, M. (2018). Assessment of Hydrogeochemical Status of Groundwater in a Coastal Region of Southeast Coast of India. *Applied Water Sciences, 8,* Article No. 27. https://doi.org/10.1007/s13201-018-0649-2

Daniele, L., Tardani, D., Schmidlin, D., Quiroga, I., Cannatelli, C., & Somma, R. (2022). Seawater Intrusion and Hydrogeochemical Processes in the Ischia Island Groundwater System. *Journal of Geochemical Exploration, 234,* Article ID: 106935. https://doi.org/10.1016/j.gexplo.2021.106935

De Montety, V., Radakovitch, O., Vallet-Coulomb, C., Blavoux, B., Hermitte, D., & Valles, V. (2008). Origin of Groundwater Salinity and Hydrogeochemical Processes in a Confined Coastal Aquifer: Case of the Rhône Delta. *Applied Geochemistry, 23,* 2337-2349. https://doi.org/10.1016/j.apgeochem.2008.03.011

Diaw, M. T., Cissé-Faye, S., Gaye, C. B., Niang, S., Pouye, A., Campos, L. C., & Taylor, R. G. (2020). On-Site Sanitation Density and Groundwater Quality: Evidence from Remote Sensing and *in Situ* Observations in the Thiaroye Aquifer, Senegal. *Journal of Water Sanitation and Hygiene for Development, 10,* 927-939. https://doi.org/10.2166/washdev.2020.162

Diédhiou, M., Cissé Faye, S., Diouf, O. C., Faye, S., Faye, A., Re, V., Wohnlich, S., Wisotzky, F., Schulte, U., & Maloszewski, P. (2011). Tracing Groundwater Nitrate Sources in the Dakar suburban Area: An Isotopic Multi-Tracer Approach. *Hydrological Processes, 26,* 760-770. https://doi.org/10.1002/hyp.8172

Diouf, O. C., Faye, S. C., Diedhiou, M., Kaba, M., Faye, S., Gaye, C. B., Faye, A., Englert, A., & Wohnlich, S. (2012). Combined Uses of WTF, CMB and Environmental Isotopes Methods to Investigate Groundwater Recharge in the Thiaroye Sandy Aquifer (Dakar, Senegal). *African Journal of Environmental Science and Technology, 6,* 425-437. http://www.academicjournals.org/AJEST https://doi.org/10.5897/AJEST12.100

Diouf, O. C., Weihermüller, L., Ba, K., Faye, S. C., Faye, S., & Vereecken, H. (2016). Estimation of Turc Reference Evapotranspiration with Limited Data against the Penman-Monteith Formula in Senegal. *Journal of Agriculture and Environment for International Development, 110,* 117-137.

Dixon, W., & Chiswell, B. (1992). The Use of Hydrochemical Sections to Identify Recharge Areas and Saline Intrusions in Alluvial Aquifers, Southeast Queensland, Australia. *Journal of Hydrology, 135,* 259-274. https://doi.org/10.1016/0022-1694(92)90091-9

Eissa, M., De-Dreuzy, J., & Parker, B. (2018). Integrative Management of Saltwater Intrusion in Poorly-Constrained Semiarid Coastal Aquifer at Ras El-Hekma, Northwestern Coast, Egypt. *Groundwater for Sustainable Development, 6,* 57-70. https://doi.org/10.1016/j.gsd.2017.10.002

Fadili, A., Mehdi, K., Riss, J., Najib, S., Makan, A., & Boutayab, K. (2015). Evaluation of Groundwater Mineralization Processes and Seawater Intrusion Extension in the Coastal Aquifer of Oualidia, Morocco: Hydrochemical and Geophysical Approach. *Arabian Journal of Geosciences, 8,* 8567-8582. https://doi.org/10.1007/s12517-015-1808-5

Faye, S., Maloszewski, P., Stichler, W., Trimborn, P., Faye, S. C., & Gaye, C. B. (2005). Groundwater Salinization in the Saloum (Senegal) Delta Aquifer: Minor Elements and Isotopic Indicators. *Science of the Total Environment, 343,* 243-259. https://doi.org/10.1016/j.scitotenv.2004.10.001

Gaye, C. B. (1980). *Etude hydrogéologique, hydrochimique et isotopique de la nappe infrabasaltique de la presqu'île du Cap Vert.* Ph.D. Thesis, Université de Dakar (Sénégal).

GKW Consult (2009). *Modélisation Numérique—Aquifère Infrabasaltique*. Rapport Phase IV Lot 1A, 82 p.

Hoyle, B. L. (1990). Ground-Water Quality Variations in a Sility Alluvial Soil Aguifer, Oklahama. *Groundwater, 27,* 540-549. https://doi.org/10.1111/j.1745-6584.1989.tb01975.x

Isa, N. M., Aris, A. Z., & Sulaiman, W. N. A. W. (2012). Extent and Severity of Groundwater Contamination Based on Hydrochemistry Mechanism of Sandy Tropical Coastal Aquifer. *Science of the Total Environment, 438,* 414-425. https://doi.org/10.1016/j.scitotenv.2012.08.069

Kass, A., Gavrieli, I., Yechieli, Y., Vengosh, A., & Starinsky, A. (2005). The Impact of Freshwater and Wastewater Irrigation on the Chemistry of Shallow Groundwater: A Case Study from the Israeli Coastal Aquifer. *Journal of Hydrology, 300,* 314-331. https://doi.org/10.1016/j.jhydrol.2004.06.013

Klassen, J., Allen, D. M., & Kirste, D. (2014). *Chemical Indicators of Saltwater Intrusion for the Gulf Islands, British Columbia, Final Report.* Simon Fraser University.

Kumari, R., Datta, P. S., Rao, M. S., Mukherjee, S., & Azad, C. (2018). Anthropogenic Perturbations Induced Groundwater Vulnerability to Pollution in the Industrial Faridabad District, Haryana, India. *Environmental Earth Sciences, 77,* Article No. 187. https://doi.org/10.1007/s12665-018-7368-8

Lal, A., & Bithin, D. (2019). Multi-Objective Groundwater Management Strategy under Uncertainties for Sustainable Control of Saltwater Intrusion: Solution for an Island Country in the South Pacific. *Journal of Environmental Management, 234,* 115-130. https://doi.org/10.1016/j.jenvman.2018.12.054

Li, P., & Qian, H. (2018). Water Resources Research to Support a Sustainable China. *International Journal Water Research Development, 34,* 327-336. https://doi.org/10.1080/07900627.2018.1452723

Maman Hassan, A. (2022). Hydrogeochemical and Isotopic Investigations on the Origins of Groundwater Salinization in Çarşamba Coastal Aquifer (North Turkey). *Environmental Earth Sciences, 81,* Article No. 128. https://doi.org/10.1007/s12665-022-10248-5

Marghade, D., Malpe, D. B., & Zade, A. B. (2012). Major Ion Chemistry of Shallow Groundwater of a Fast Growing City of Central India. *Environmental Monitoring and Assessment, 184,* 2405-2418. https://doi.org/10.1007/s10661-011-2126-3

Martin, A. (1970). *Les nappes de la presqu'île du Cap-vert: Leur utilisation pour l'alimentation en eau de Dakar* (56 p). BRGM.

Meybeck, M. (1987). Global Chemical Weathering of Surficial Rocks Estimated from River Dissolved Loads. *American Journal of Science, 287,* 401-428. https://doi.org/10.2475/ajs.287.5.401

Mondal, N. C., Singh, V. S., & Rangarajan, R. (2009). Aquifer Characteristics and Its Modeling around an Industrial Complex, Tuticorin, Tamil Nadu, India: A Case Study. *Journal of Earth System Science, 118,* 231-244. https://doi.org/10.1007/s12040-009-0017-6

Moujabber, M. E. L., Samra, B. B., Darwish, T., & Atallah, T. (2006). Comparison of Different Indicators for Groundwater Contamination by Seawater Intrusion on the Lebanese Coast. *Water Resources Management, 20,* 161-180. https://doi.org/10.1007/s11269-006-7376-4

Narayana, A., & Suresh, G. (1989). Chemical Quality of Groundwater of Mangalore City, Karnataka. *Indian Journal of Environmental Health, 31,* 228-236.

OMS (1972). *Approvisionnement en eau et Assainissement de Dakar et ses environs. Etude des souterraines, Tome II: Nappes des Quaternaires* (139 p). OMS.

Pascual, M., & Custodio, E. (1990). Geochemical Observation in a Continuously Seawater Intruded Area: Garraf, Catalonia (Spain). In 11*th Saltwater Intrusion Meeting* (pp. 308-330). IAHS.

Piper, A. M. (1944). A Graphic Procedure in the Geochemical Interpretation of Water-Analyses. *Eos, Transactions American Geophysical Union, 25,* 914-928. https://doi.org/10.1029/TR025i006p00914

Pouye, A., Faye, S. C., Diedhiou, M., Gaye, C. B., & Taylor, R. G. (2022). An Evaluation of Groundwater Vulnerability Assessment Methods in a Rapidely Urbanizing City: Evidence from Dakar, Senegal. *Environmental Earth Sciences, 81,* Article No. 410. https://doi.org/10.1007/s12665-022-10531-5

Prakash, R., Srinivasamoorthy, K., Gopinath, S., Saravanan, K., & Vinnarasi, F. (2020). Hydrogeochemical Investigations to Assess Groundwater and Saline Water Interaction in Coastal Aquifers of the Southeast Coast, Tamil Nadu, India. *Environmental Science and Pollution Research, 28,* 5495-5519.

https://doi.org/10.1007/s11356-020-10870-5

Pulido-Leboeuf, P. (2004). Seawater Intrusion and Associated Processes in a Small Coastal Complex Aquifer (Castell de Ferro, Spain). *Applied Geochemistry, 19,* 1517-1527. https://doi.org/10.1016/j.apgeochem.2004.02.004

Putra, D. B. E., Hadian, M. S. D., Alam, B. Y. C. S., Yuskar, Y., Yaacob, W. Z. W., Datta, B., & Harnum, W. P. D. (2021). Geochemistry of Groundwater and Saltwater Intrusion in a Coastal Region of an Island in Malacca Strait, Indonesia. *Environmental Engineering Research, 26,* Article ID: 200006. https://doi.org/10.4491/eer.2020.006

Ramesh, R., Shiv Kumar, K., Eswaramoorthy, S., & Purvaja, G. R. (1995). Migration and Contamination of Major and Trace Elements in Groundwater of Madras City, India. *Environmental Geology, 25,* 126-136. https://doi.org/10.1007/BF00767869

Revelle, R. (1941). Criteria for Recognition of Sea Water in Ground-Waters. *Eos, Transactions American Geophysical Union, 22,* 593-597. https://doi.org/10.1029/TR022i003p00593

Rogers, R. J. (1989). Geochemical Comparison of Groundwater in Areas of New England, New York, and Pennsylvania. *Groundwater, 27,* 690-712. https://doi.org/10.1111/j.1745-6584.1989.tb00483.x

Rosegrant, M. W., Ringler, C., & Zhu, T. (2009). Water for Agriculture: Maintaining Food Security under Growing Scarcity. *Annual Review of Environment Resources 34,* 205-222. https://doi.org/10.1146/annurev.environ.030308.090351

Roy, D. K., & Bithin, D. (2018). A Review of Surrogate Models and Their Ensembles to Develop Saltwater Intrusion Management Strategies in Coastal Aquifers. *Earth Systems and Environment, 2,* 193-211. https://doi.org/10.1007/s41748-018-0069-3

Sami, K. (1992). Recharge Mechanisms and Geochemical Processes in a Semi-Arid Sedimentary Basin, Eastern Cape, South Africa. *Journal of Hydrology, 139,* 27-48. https://doi.org/10.1016/0022-1694(92)90193-Y

Sawyer, G. N., & McCartly, D. L. (1967). *Chemistry of Sanitary Engineers* (2nd ed., p. 518). McGraw-Hill.

Saxena, V. K., Mondal, N. C., & Singh, V. S. (2004). Evaluation des paramètres hydrogéochimiques pour délimiter les zones d'eau douce dans les aquifères côtiers. *Journal of Applied Geochemistry, 6,* 245-254.

Schiavo, M. A., Hauser, S., Cusimano, G., & Gatto, L. (2006). Geochemical Characterization of Groundwater and Submarine Discharge in the South-Eastern Sicily. *Continental Shelf Research, 26,* 826-834. https://doi.org/10.1016/j.csr.2005.12.001

Srinivas, Y., Hudson Oliver, D., Stanley Raj, A., & Chanderasekar, N. (2013). Evaluation of Groundwater Quality in and around Nagercoil Town, Tamilnadu, India: An Integrated Geochemeical and GIS Approach. *Applied Water Sciences, 3,* 631-651. https://doi.org/10.1007/s13201-013-0109-y

Stuyfzand, P. J. (2008). Base Exchange Indices as Indicators of Salinization or Freshening of (Coastal) Aquifers. In 20*th Saltwater Intrusion Meeting* (pp. 262-265). IFAS Research.

Tandia, A. A. (2000). *Origine, évolution et migration des formes de l'azote minéral dans les aquifères situés sous environnement périurbain non assaini: Cas de la nappe des sables quaternaires de la région de Dakar (Sénégal)* (208 p). Ph.D. Thesis, Université Cheikh Anta de Dakar.

Tandia, A. A., Gaye, C. B., & Faye A. (1998). *Origin, Process and Migration of Nitrate Compounds in the Aquifer of Dakar Region, Senegal* (pp. 67-80). International Atomic Energy Agency.

Todd, D. K. (1980). *Groundwater Hydrology* (2nd ed.). Wiley.

Todd, D. K., & Larry, W. M. (2005). *Groundwater Hydrology* (3rd ed.). John Wiley & Sons.

Walraevens, K., & Van Camp, M. (2005). Advances in Understanding Natural Groundwater Quality Controls in Coastal Aquifers. In *Proceedings of the 18th Salt Water Intrusion Meeting (SWIM)* (pp. 451-460). Instituto Geologico y Minero de España.

Werner, A. D., Hannah, K. S., Sandra, C. G., Post, V. E. A., & Sinclair, P. (2017). Hydrogeology and Management of Freshwater Lenses on Atoll Islands: Review of Current Knowledge and Research Needs. *Journal of Hydrology, 551,* 819-844. https://doi.org/10.1016/j.jhydrol.2017.02.047

WHO (2017). *Guidelines for Drinking-Water Quality: Fourth Edition, Incorporating the First Addendum* (541 p.). World Health Organization.